PHYSICAL REVIEW E, VOLUME 64, 020101(R)

# Description of random Gaussian surfaces by a four-vertex model

Jaan Kalda
*Institute of Cybernetics, Tallinn Technical University, Akadeemia tee 21, 12618 Tallinn, Estonia*
(Received 6 June 2000; published 19 July 2001)

A lattice model of random self-affine surfaces is derived using the inverse order of applying the six-vertex model. The well-argued simplification of such an approach results in the four-vertex model. The high numerical efficiency of the four-vertex model is demonstrated by calculating the fractal dimension of contour loops (isolines) of fractional Brownian surfaces as the function of the roughness exponent.

DOI: 10.1103/PhysRevE.64.020101 PACS number(s): 05.40.−a, 64.60.Ak, 68.35.Bs, 91.10.Jf

Various physical phenomena can be modeled by random Gaussian surfaces, which are scale-invariant within a wide range of scales. Here are few examples: geological landscapes [1], deposited metal films [2], fractured surfaces [3,4], streamfunctions of two-dimensional (2D) turbulent flows [5] (particularly, several scaling laws of the passive scalar turbulence have been expressed via the fractal dimensions of the streamfunction contour loops [6,7]). Such surfaces have been observed and studied in many experiments, cf. references in [2,3]; their generic statistical properties have been studied both analytically and numerically [2–6,8–10].

Here we develop a simple *four-vertex* (4V) model providing an easy way to produce lattice representations of rough surfaces with specified statistical properties. This model can be used as a universal and efficient tool for numerical simulations, as evidenced below by calculating the fractal dimension of contour loops of self-affine surfaces.

The structure of the paper is as follows. First, we derive the *inverse six-vertex model* as a generalization of the 2D percolation model. This model maps random surfaces to 2D lattices and is similar to the six-vertex (6V) model [11] (hence the name of the model). Further we focus on the 4V model, which is the 1+1-dimensional [(1+1)D] version of the inverse 6V model. It is argued that the (1+1)D surfaces of the 4V model belong to the same universality class (i.e. obey the same scaling laws) as the statistically isotropic two-dimensional surfaces. This simplified (1+1)D geometry results in a very high numerical efficiency of the 4V model.

It has been known for a long time that the statistical topography of the *"monoscale"* surfaces can be mapped to the (possibly correlated) percolation problem on irregular lattices [12,13]. The term ''monoscale'' refers to the smooth surfaces of bounded $\Delta$ variance $\Delta(\boldsymbol{r}_0)=\langle[\psi(\boldsymbol{r})-\psi(\boldsymbol{r}+\boldsymbol{r}_0)]^2\rangle$ and decaying correlation function $C(\boldsymbol{r}_0)=\langle\psi(\boldsymbol{r})\psi(\boldsymbol{r}+\boldsymbol{r}_0)\rangle$. Here the function $\psi(\boldsymbol{r})$ defines the height of a surface, and $\boldsymbol{r}$ is a vector on the reference plane. If the long-scale decay rate of $C(\boldsymbol{r}_0)$ is high [more specifically, at the limit $r\to\infty$, $C(\boldsymbol{r}_0)<r^{-3/4}$], then the problem belongs to the universality class of ordinary percolation [14]. Otherwise we are dealing with the correlated percolation problem [15], when the critical exponents depend on the scaling exponent of the correlation function. The mapping of Ziman [12,13] can be also adapted to the *"multiscale" surfaces* of unbounded delta variance (cf. [3]), particularly to the *fractional Brownian surfaces* [16] with $\Delta(\boldsymbol{r}_0)\propto|\boldsymbol{r}_0|^{2H}$, where $H$ is the Hurst (or roughness) exponent. However, in this case a more efficient approach can be developed by making use of the mapping between the 6V model and the body-centered solid-on-solid (SOS) model [17,18]. Its main advantage is that a complete set of equidistant horizontal contour cuts can be generated at once on a single lattice. This is a particularly useful feature for the numerical analysis of passive scalar transport [10].

The mapping developed in [12,13] can be outlined as follows. The minima $m_i$ of the random surface define the sites of an irregular percolation lattice. The saddle-points $S_{ij}$ [between $i$th and $j$th minima $(i<j)$] correspond to the bonds of the lattice. Thus, the bonds can be drawn as the steepest descend paths from $S_{ij}$ to $m_i$ and $m_j$, see Fig. 1. The dual lattice is constructed analogously; its sites (and hence the faces of the primary lattice) correspond to the maxima $M_i$ of the surface. Suppose now that the random surface is flooded by water. If the water level $\psi_0$ is low, only the minima are flooded. Two neighboring ''lakes'' $m_i$ and $m_j$ become connected by a ''strait,'' when the flood level $\psi_0$ reaches the saddle-point $S_{ij}$. Therefore, the lattice bond is declared unbroken if $\psi(S_{ij})<\psi_0$, where $\psi(S_{ij})$ is the surface height at the saddle point; this criterion is equivalent to (possibly correlated) dicing at every bond. Then, the flooded regions

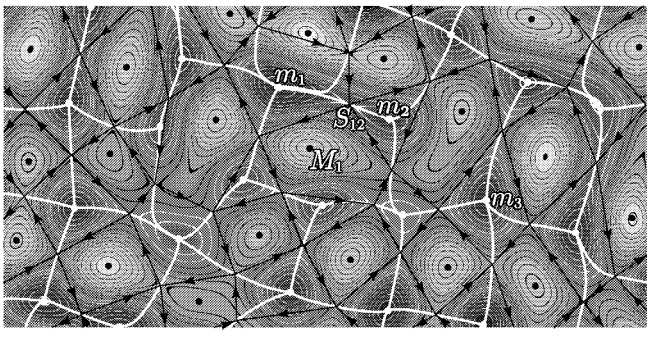


FIG. 1. Mapping of the continuous percolation problem to the percolation on an irregular lattice. Black and white loops are level lines of the random surface, lower regions are darker; black dots denote the maxima, and white dots, the minima. Black lines with arrows form the surrounding lattice; their crossing points are the saddles of the surface. The percolation lattice itself is formed by bold white lines, which are the steepest descend paths from the saddle points to the minima.

 

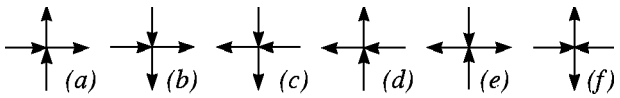


FIG. 2. Possible arrow configurations for the six-vertex model.

correspond to the percolation clusters, and the flood level $\psi_0$ matches the fraction of unbroken bonds.

Further, the surface height $\psi(\boldsymbol{r})$ can be interpreted as the stream function of a velocity field $\boldsymbol{v}=\hat{\boldsymbol{z}}\times\nabla\psi(\boldsymbol{r})$; here $\hat{\boldsymbol{z}}$ denotes the unit vector perpendicular to the reference plane. Then, the sites and faces of the percolation lattice represent the elementary vortices of opposite polarity. The direction of the flow can be marked by arrows along the edges of the surrounding lattice (the sites of which are defined as the midpoints of the bonds and edges, as the lines separating the sites of the primary lattice from the sites of the dual lattice). The vertices of the surrounding lattice correspond to the saddle points of the surface, and each vertex meets four edges representing the fluxes of the velocity field between neighboring minima and maxima. These fluxes can be assumed to be of the unit length. Indeed, with a proper choice of units, all the extrema can be put equal to $\pm 0.5$ without affecting the behavior of the long contour lines (which are always close to the percolation level $\psi=0$) by deforming the surface in the neighborhood of the extrema. The hulls (the loops of arrows surrounding tightly the percolation clusters) correspond to the contour lines $\psi(\boldsymbol{r})=\psi_0$.

This mapping can be applied to the ''multiscale'' surfaces, as well [3]. However, the criterion $\psi(S_{ij})<\psi_0$ is no more equivalent to dicing. Indeed, the heights of the saddle points of an infinitely extending ''multiscale'' surface vary in an unbounded range. Meanwhile, the height difference of neighboring saddle points remains finite. Such a distribution of heights cannot be obtained as a result of dicing. Besides, the pattern of arrows on the surrounding lattice is no more equivalent to the original surface. The heights of the extrema of the ''multiscale'' surfaces vary also in an unbounded range and cannot be put equal to $\pm 0.5$. Thus, the fluxes are unavoidably of different strength, and for a complete mapping, each arrow on the surrounding lattice has to be labeled with the respective number.

The *inverse six-vertex model* restores the situation when all the arrows on the surrounding lattice are of unit length by abandoning the one-to-one mapping between the saddle points of the surface and the vertices of the surrounding lattice (the other mapping pairs are also lost). Instead, the streamfunction $\psi(\boldsymbol{r})$ is approximated by such a discrete function, which is defined at the faces of an arbitrary (e.g., quadratic) surrounding lattice and has face-to-face increments either $+1$ or $-1$ (reasonable fit of real physical surfaces can be achieved by a proper choice unit lengths). As a result, all the interface fluxes are unitary and *the arrows on the surrounding lattice provide a complete representation of the surface*. Due to incompressibility, at each vertex, there are two incoming and two outgoing arrows, i.e., the arrows can be oriented in six different ways, exactly like in the case of six-vertex model, see Fig. 2. However, the six-vertex model is a statistical model, which ascribes a certain Hamiltonian to

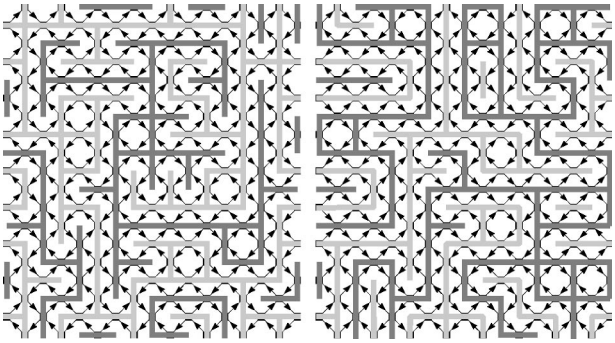

FIG. 3. Percolation (left) and inverse six-vertex (right) models: dark gray lines depict the percolation clusters, and light gray lines, the bonds of the dual lattice. The arrows on the surrounding lattice (diagonal grid) can be treated as unitary fluxes of an incompressible flow. The oriented loops of arrows are the cluster hulls and represent the level lines of the streamfunction. For the percolation model, the flow is formed by regularly packed elementary vortices. For the inverse six-vertex model, the polarity of vortices (the direction of arrows) is shuffled; the scaling exponents are defined by long-range correlation of the direction of the arrows.

the configuration of arrows. According to the conventional model [11], all the arrow configurations are taken with equal weights; the corresponding surface has roughness exponent $H=0$ [17]. Here we are proceeding in an *inverse order*: if there is a surface (or an ensemble of surfaces with specified statistical properties), then the *inverse six-vertex model* provides a convenient and numerically efficient way to construct a lattice representation of it.

For the percolation model, all the vertices of the surrounding lattice are saddlelike: counting the edges in the clockwise order, the incoming and outgoing arrows are alternating [patterns (e) and (f) in Fig. 2; thus, the percolation model could also have been named the two-vertex model]. Here we have also some shearlike vertices: two outgoing arrows are followed by two incoming ones [patterns (a)–(d) in Fig. 2]. Hence, the inverse six-vertex model can be considered as a generalization of the percolation model. The clusters (dark gray lines in Fig. 3) are the regions with $2n-0.5<\psi(\boldsymbol{r})\leqslant 2n+0.5$, where $n$ is an integer. For a shearlike vertex, the bond is kept, if on both sides of it, there is one incoming and

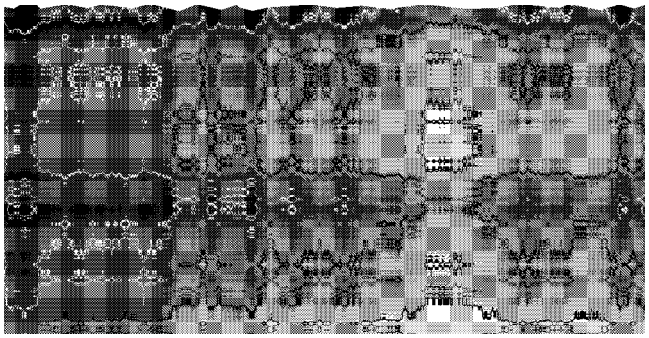

FIG. 4. Four-vertex (1+1-dimensional) model: a pattern arising for the polygon size $L=2049$ and $H=0.5$. Darker areas correspond to lower regions of the surface; black and white lines depict equidistant level lines.

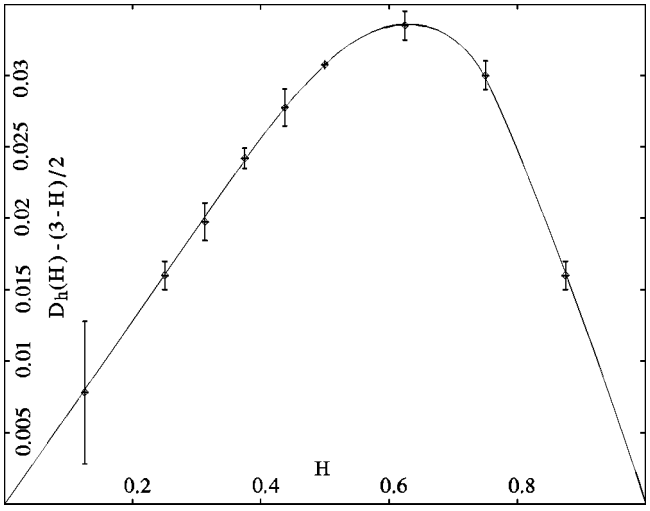


FIG. 5. Difference between the fractal dimension of the contour loops and the linear conjecture $D_{\mathrm{lin}}=(3-H)/2$.

one outgoing arrow. For a saddlelike vertex, the fate of the bond is defined by the actual height of the saddle point, exactly like in the case of the percolation model [more precisely, since one-to-one mapping between the saddle points and bonds has been lost, the bond between two vertices is kept, if the vertices are connected by region $2n-0.5<\psi(\boldsymbol{r}) \leqslant 2n+0.5$]. In Fig. 3, the saddle heights are continuously distributed. However, for the sake of simplicity, one can also simply break (keep) all these bonds by slightly deforming the surface: the scaling laws will not be affected, since the required change in the surface height is small ($<0.5$). Note also that the clusters and hulls [the level lines $\psi(\boldsymbol{r})=2n \pm 0.5$] have the same fractal dimension: each cluster is embraced between two hulls of a small average distance [their level difference (one) is much less than the large-scale variance (unbounded)].

The inverse 6V model can be easily applied to study the properties (e.g., the statistics of contour loops) of *natural surfaces*. However, the Monte Carlo analysis of random *model surfaces* (e.g., fractional Brownian surfaces) can be very time-consuming. Such calculations can be greatly simplified by using (1+1)D geometry [10]. The real 2D stream function $\psi(x,y)$ is substituted by the stream function of two shear flows $\psi_1(x)-\psi_2(y)$; see Fig. 4. Here $\psi_{1,2}(x)$ are random functions of one variable obeying the same statistical properties as the function $\psi(x,0)$. It has been expected that for fractional Brownian functions, both surfaces belong to the same universality class, i.e., the scaling exponents are the same. There are several reasons for such an expectation: (a) in both cases, the scaling laws of the correlation function and delta variance are the same; (b) in both cases, the fractal dimension of the complete set of contour loops at a fixed height is $D=2-H$ [1]; (c) according to the numerical results for $H=0.5$, the fractal dimension of a single contour loop $D_h=1.281\pm0.003$ remains unchanged, when the quasi-2D flow is made up of more than two shear flows [10].

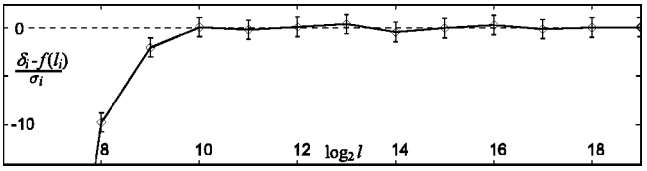


FIG. 6. Displacement vs the curve length of contour loops in 1+1-dimensional geometry, $H=0.5$. The mismatch between the numerical results $\delta_i$ and fitted function $f(l_i)$ is reduced to the standard deviation $\sigma_i$.

In the case of (1+1)D surfaces, the inverse six-vertex model becomes extremely simple. There are no more saddlelike vertices of the surrounding lattice, i.e., of the six possible arrow configurations, two are excluded. This allows us to speak about a *four-vertex model*. On the square lattice, the contour lines can be found according to the following algorithm:

$$x_{n+1}=x_n+\varphi_2(y_n), \quad y_{n+1}=y_n+\varphi_1(x_{n+1}). \tag{1}$$

Here $(x_n,y_n)$ are the coordinates of the $n$th point on a contour line (hull); $\varphi_1(x),\varphi_2(y)=\pm1$ are the increments of the streamfunction (in the case of $H=0.5$ — random uncorrelated sequences of $+1$ and $-1$).

Algorithm (1) was used to calculate the fractal dimension of the contour line as the function of the roughness exponent $H$; see Fig. 5. The average distance $\delta=\langle\max(|x_a-x_b|,|y_a-y_b|)\rangle$ between the endpoints $\boldsymbol{r}_{a,b}$ of the contour line segments of length $l$ was determined for different values of $l$ using the Monte Carlo method. The fractal dimensions were found using least square fit of the direct simulation results, see Fig. 6. The asymptotic behavior $\delta\rightarrow Al^{1/D_h}+Bl^{C}$ was expected; an alternative fitting function $\delta\rightarrow Al^{1/D_h}+Bl^{-1+1/D_h}+C$ was also tested. For $H=0$, the correction to the fractal scaling $\delta\rightarrow Al^{1/D_h}$ appeared to be more complex than a simple power law [19]; this is the cause of a relatively high uncertainty. Except for $H=0.5$, the computer time needed to generate a single contour line of length $l$ is determined by the time needed to produce a fractional Brownian time series of length $\delta$ and scales as $\delta^2$. For $H=0.5$, there is no need to generate fractional Brownian function (which is substituted by simple Brownian function); the computation time scales simply as the length of the curve $l$. Owing to this, it was possible to determine the fractal dimension with a very high precision, $D_h(H=0.5)=1.280\,75\pm0.000\,05$.

These results do not support the super-universality hypothesis of Kondev and Henley [8], which, if valid, would lead to the analytic dependence $D_h(H)=(3-H)/2$, i.e., to a simple horizontal line in Fig. 5. For $H=0.5$, there is a good agreement between our result and that of Apelian *et al.* [10]. The good agreement between our estimate $D_h(H=0)=1.50\pm0.01$ and the analytic 2D result $D_h(0)=1.5$ [20,8] serves as an additional argument supporting the idea that (1+1)D and 2D surfaces belong to the same universality class.

In conclusion, the four-vertex model is a numerically efficient [see Eq. (1)] lattice model of the multiscale surfaces, applicable to various physical phenomena. It is particularly well-suited for the analysis of passive scalar transport in turbulent velocity field. Our simulation results (i) support the idea that (1+1)D and 2D fractional Brownian surfaces belong to the same universality class; (ii) call in question the super-universality hypothesis [8] and hence the formula $D_h = (3-H)/2$.

The support of Estonian Science Foundation Grant No. 3739 is acknowledged. The author is grateful to Professor J. Engelbrecht for useful discussions.

[1] B. B. Mandelbrot, *The Fractal Geometry of Nature* (Freeman, New York, 1982).
[2] J. Kondev, C. L. Henley, and D. G. Salinas, Phys. Rev. E **61**, 104 (2000).
[3] M. Sahimi, Phys. Rep. **306**, 213 (1998).
[4] E. Bouchaud, G. Lapasset, J. Planès, and S. Naveos, Phys. Rev. B **48**, 2917 (1993).
[5] M. B. Isichenko, Rev. Mod. Phys. **64**, 961 (1992).
[6] M. B. Isichenko and J. L. Kalda, J. Nonlinear Sci. **1**, 255 (1991).
[7] J. Kalda, In *Transport, Chaos and Plasma Physics*, edited by S. Benkadda, F. Doveil, and Y. Elskens (World Scientific, Singapore, 1994), p. 272.
[8] J. Kondev and C. L. Henley, Phys. Rev. Lett. **74**, 4580 (1995).
[9] Z. Olami and R. Zeitak, Phys. Rev. Lett. **76**, 247 (1996).
[10] C. Apelian, R. L. Holmes, and M. Avellaneda, Commun. Pure Appl. Math. **50**, 1053 (1997).
[11] F. Rys, Helv. Phys. Acta **36**, 537 (1963).
[12] J. M. Ziman, J. Phys. C **1**, 1532 (1969).
[13] A. Weinrib, Phys. Rev. B **26**, 1352 (1982).
[14] S. R. Broadbent and J. M. Hammersley, Biol. Rev. Camb. Philos. Soc. **53**, 629 (1957).
[15] A. Weinrib, Phys. Rev. B **29**, 387 (1984).
[16] B. B. Mandelbrot and J. W. Van Ness, SIAM Rev. **10**, 422 (1968).
[17] H. van Beijeren, Phys. Rev. Lett. **38**, 993 (1977).
[18] P. Meakin, P. Ramanlal, L. M. Sander, and R. C. Ball, Phys. Rev. A **34**, 5091 (1986).
[19] J. Kalda (unpublished).
[20] H. Saleur and B. Duplantier, Phys. Rev. Lett. **58**, 2325 (1987).